

PRE-COSTAR FOS APERTURE THROUGHPUTS FROM MODELS

I. N. Evans

Space Telescope Science Institute

FOS Instrument Science Report CAL/FOS-105

September 1993

Abstract

Monochromatic pre-COSTAR aperture throughputs for the FOS have been computed at every 200Å in wavelength from model point spread functions. Model absolute aperture throughputs and aperture throughput ratios relative to the 4.3 aperture are presented. The model aperture throughput ratios agree with the observed values on the red side, but increasingly disagree with the observed values for the smaller blue side apertures. This may be due to target mis-centering when the blue side observational data were obtained.

I. Pre-COSTAR FOS Aperture Throughputs

FOS blue side and red side pre-COSTAR monochromatic aperture throughputs have been determined for each of the non-occulting FOS apertures from the model point spread functions (PSFs) described by Evans (1993). Blue side aperture throughputs were computed for wavelengths every 200Å from 1200Å to 5400Å for the FOS blue side, and every 200Å from 1600Å to 8400Å for the FOS red side. The PSFs were computed using the default aberrations and nominal focus for the date June 1, 1993. The focus dependence of the aperture throughputs is not considered in this report. Lindler & Bohlin (1993) have considered the focus dependence of the aperture throughputs. However, their PSF models do not use the same set of parameters as, and have coarser spatial and wavelength sampling than the models employed here. Therefore it may not be possible to compare directly the model aperture throughputs of Lindler & Bohlin (1993) with the results of this report. An analysis of the focus dependence using the same model parameters as those employed herein will be described in a future report.

The aperture throughputs are defined as the ratio of the transmitted integrated flux from a point source that is perfectly centered in the aperture to the total integrated flux in the PSF at the location of the aperture. They were computed by summing the individual contributions of the PSF pixels at each pixel position within the relevant FOS aperture, and dividing this value by the total flux in the PSF. The total flux in each PSF model is computed by TIM, and is defined such that the integral of the model PSF to infinite radius is normalized to unity. Thus, the flux in each PSF model integrated outwards to a finite radius determined by the total size of the model array is slightly less than unity. For the PSFs used here, the model array flux sums to ~93–94% of the total flux integrated to infinite radius. Because of the fine pixel sampling of the PSFs, no correction for the presence of fractional pixels within a given aperture was applied. The

apertures were assumed to be perfectly circular in the case of the circular apertures, and perfectly rectangular with sides aligned precisely in the X and Y directions for the rectangular apertures. The aperture sizes used were obtained from the PDB (Dressel & Harms, unpublished), except in the cases of the 4.3 and 0.25×2.0 apertures, where the Y extent (only) of the apertures is limited by the effective diode height and was assumed to be precisely $1''43$. It is noted here that the PDB values for the aperture areas do not agree (by up to $\sim 40\%$ for the blue side 0.1-PAIR and red side 0.1-PAIR-A apertures) with pre-flight measurements of Lindler, Bohlin, and Hartig (1985).

II. Results

Absolute aperture throughputs are presented in Figure 1, where a spline fit to the individual values at each wavelength has been used to approximate the throughput as a function of wavelength. Because the absolute aperture throughputs cannot be determined observationally independently of detector sensitivity, aperture throughput ratios relative to the 4.3 aperture are presented in Figure 2. The aperture throughput ratios are independent of the detector sensitivity and so can be compared directly to observation. In Figure 2, the mean aperture throughput ratios measured for the 1.0, 0.5, 0.3, and 0.25×2.0 red side and blue side FOS apertures by Neill, Bohlin, & Hartig (1992) are indicated by open squares. Since the values provided by Neill, Bohlin, & Hartig are the mean values for each grating, they have been plotted in the figure at the effective mean wavelength of the appropriate grating as seen by the detector. The observed values given by Neill, Bohlin, & Hartig are not corrected for focus error, but this correction is small ($\lesssim 3\%$, Bohlin, private communication).

Inspection of the figure shows good agreement between the model throughput ratios and the observed throughput ratios for the red side. However, on the blue side the agreement is good for the largest aperture, but gets progressively worse as the aperture size decreases. The measured throughput ratios fall progressively below the predictions as the aperture size is decreased. Target mis-centering during the blue side observation could give rise to the observed behavior, since the light loss for a mis-centered target would be greater for smaller apertures. However, there is no independent evidence that the target was mis-centered during the blue side observation.

The absolute and relative aperture throughputs are dependent only on (a) wavelength, (b) the aperture size and shape, and (c) the point spread function profile at the location of the aperture center in the focal plane. Since for a given wavelength both items (b) and (c) generally agree to within a few percent, then the blue and red side aperture throughput ratios should similarly agree to within a few percent. This is indeed the case for the theoretical models, where the variation between the blue and red side aperture throughput ratios is typically $\lesssim 3\%$, except for the 0.1-PAIR apertures blueward of $\sim 3000\text{\AA}$, where variations of up to $\sim 30\%$ are predicted. The observationally determined aperture throughput ratios of Neill, Bohlin, & Hartig vary by up to $\sim 30\%$ between the blue side and red side measurements for the 0.3/4.3 aperture throughput ratio. The predicted maximum variation between the blue side and red side for this aperture throughput ratio is only $\sim 3.7\%$. Such a large disagreement between the observed blue side and

red side aperture throughput ratios reported by Neill, Bohlin, & Hartig suggests that the values presented in CAL/FOS-077 for the blue side may be in error.

References

- Dressel, L. & Harms, R. unpublished, FOS Instrument Science Report CAL/FOS-072
Evans, I. N. 1993, FOS Instrument Science Report CAL/FOS-104
Lindler, D. J. & Bohlin, R. C. 1993, FOS Instrument Science Report CAL/FOS-102
Lindler, D. J., Bohlin, R. C., & Hartig, G. F. 1985, FOS Instrument Science Report CAL/FOS-019
Neill, J. D., Bohlin, R. C., & Hartig, G. 1992, FOS Instrument Science Report CAL/FOS-077

Figure Captions

Fig. 1 — Absolute aperture throughputs. Each panel is identified by detector and aperture id. The continuous curve is a spline fit to the model absolute aperture throughputs computed every 200Å.

Fig. 2 — Relative aperture throughputs. Each panel is identified by detector and aperture id. The continuous curve is a spline fit to the model aperture throughputs relative to the throughput of the 4.3 aperture, computed every 200Å. Where available, observational measurements are indicated by open squares.

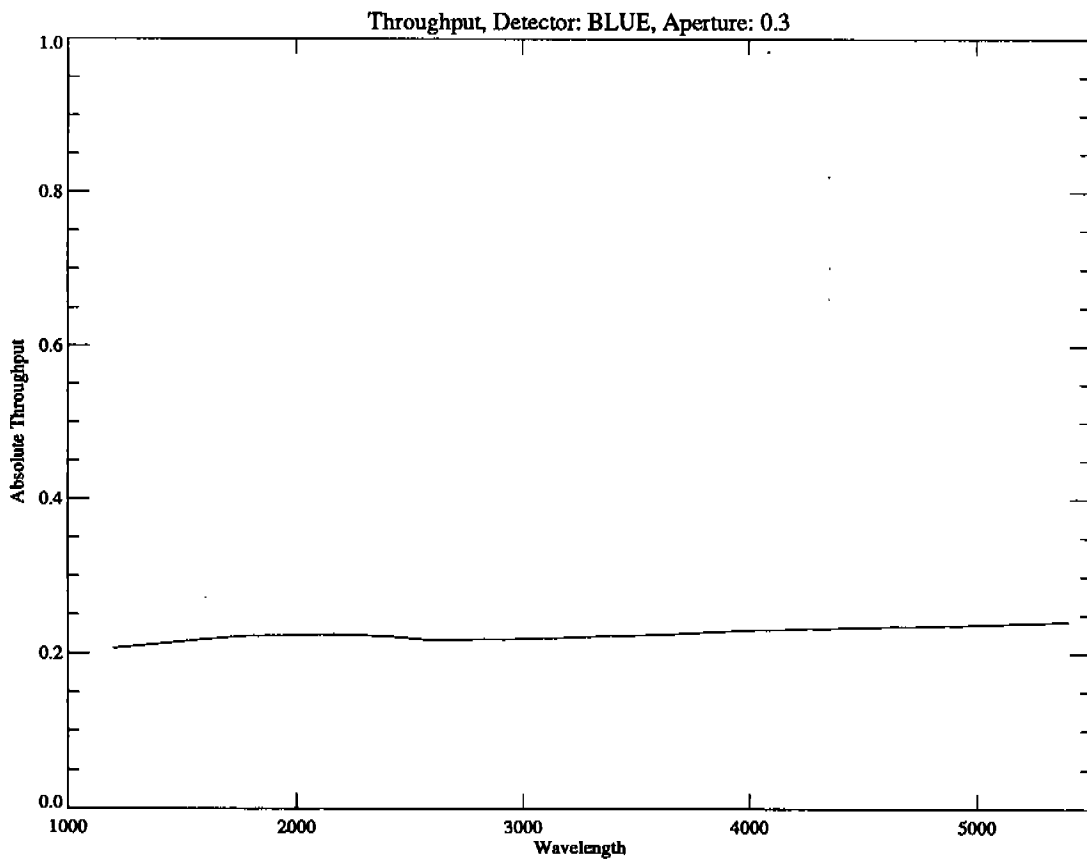
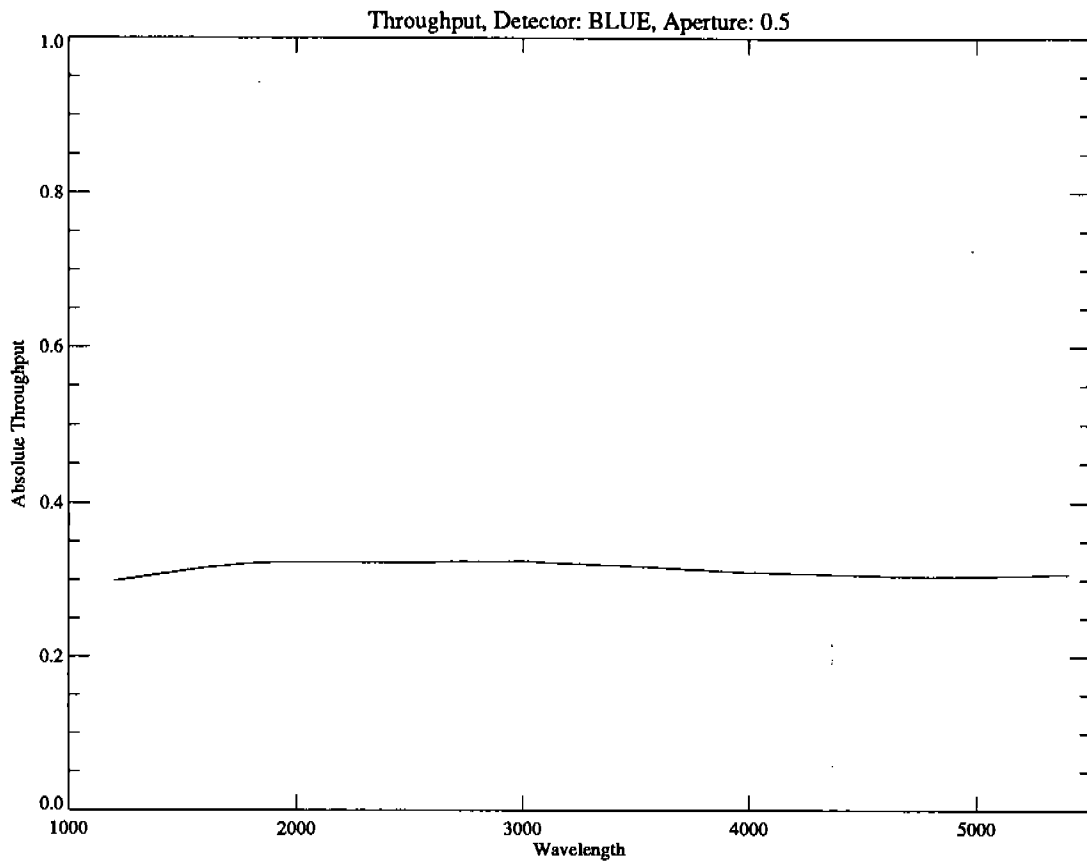


Figure 1

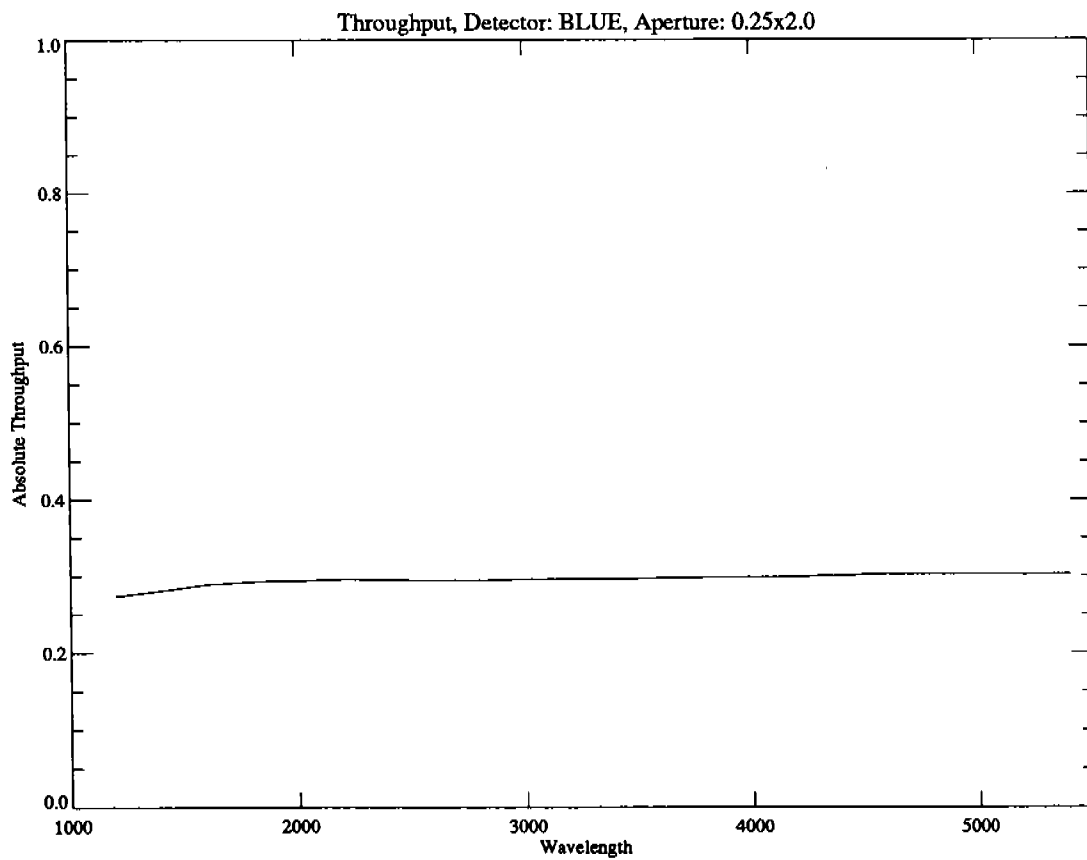
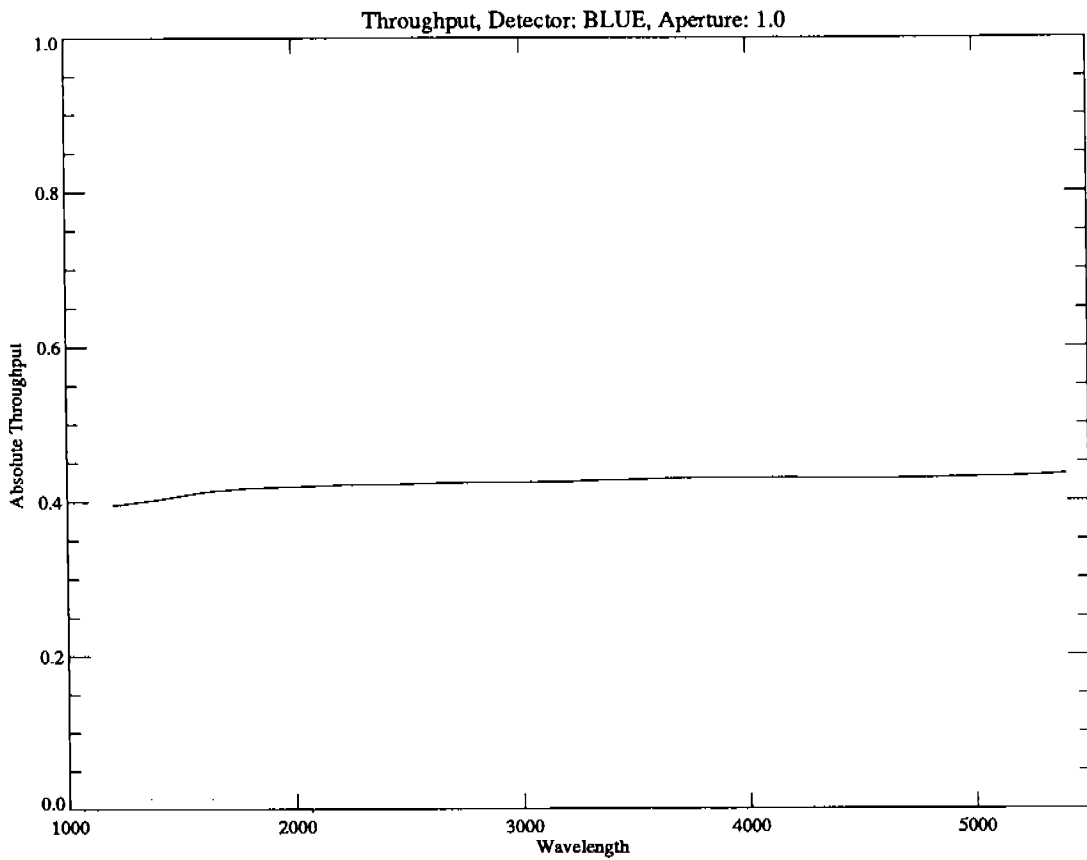


Figure 1 (Continued)

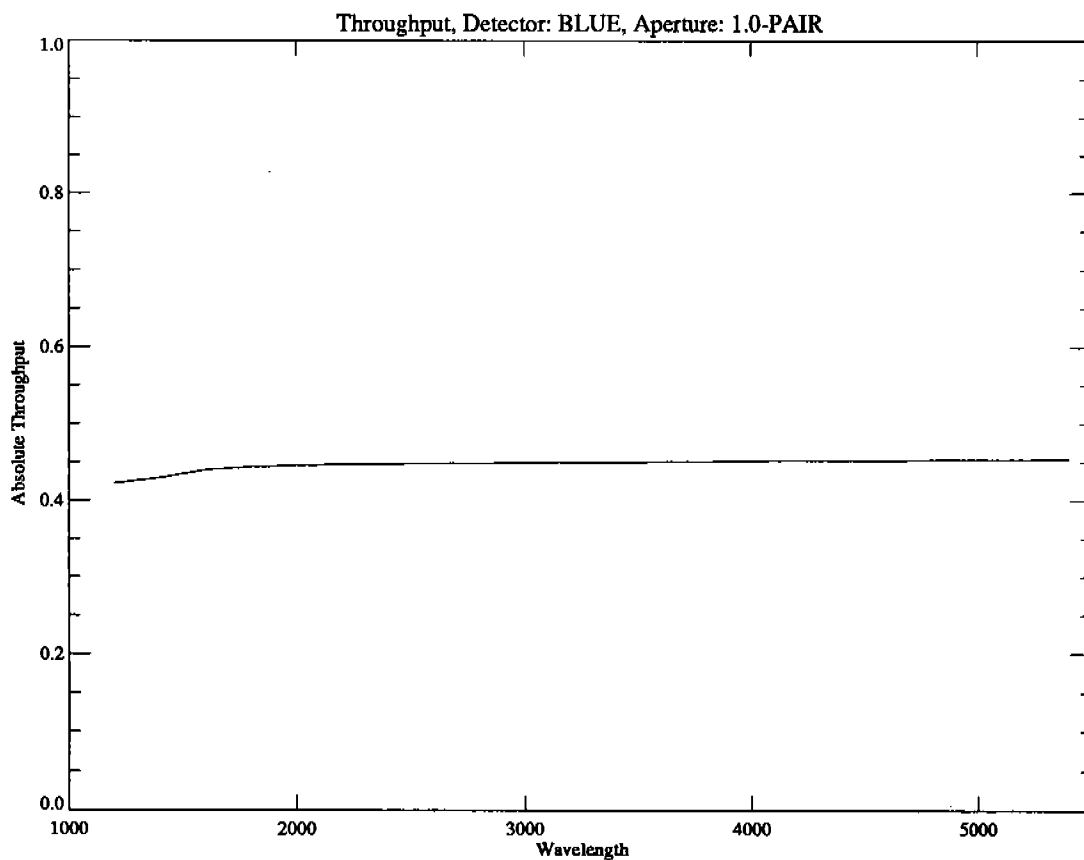
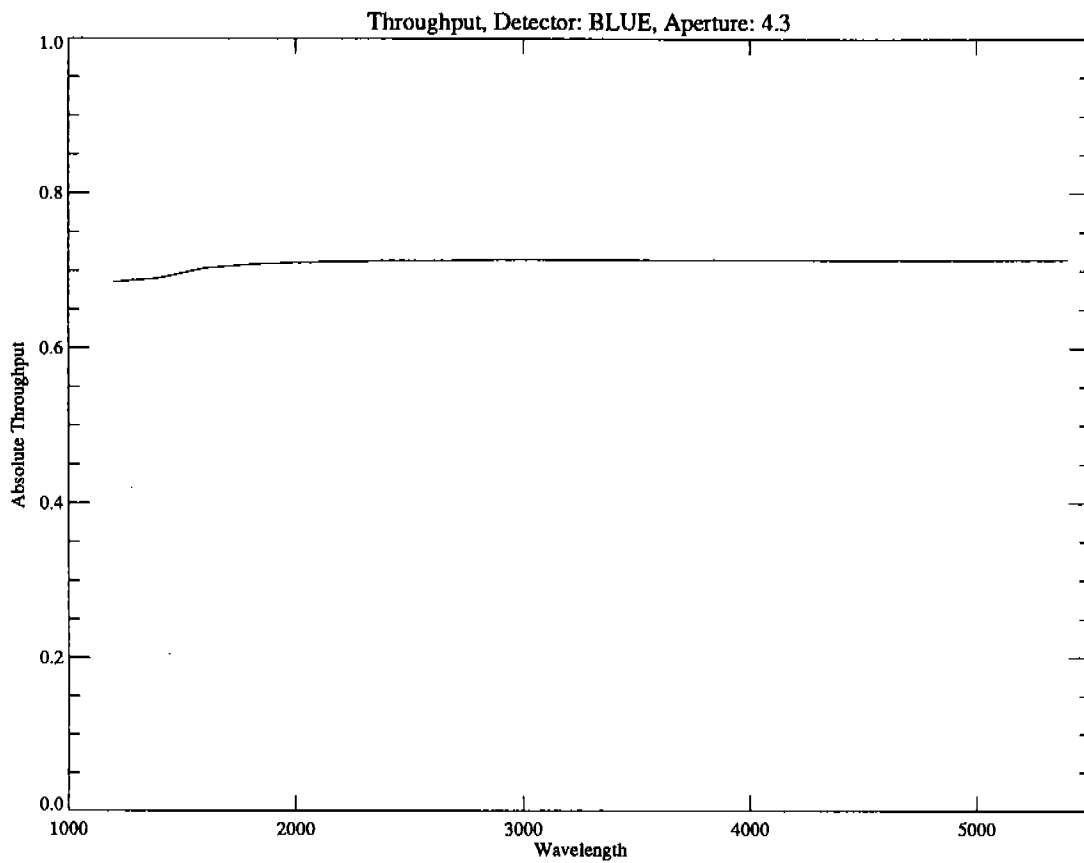


Figure 1 (Continued)

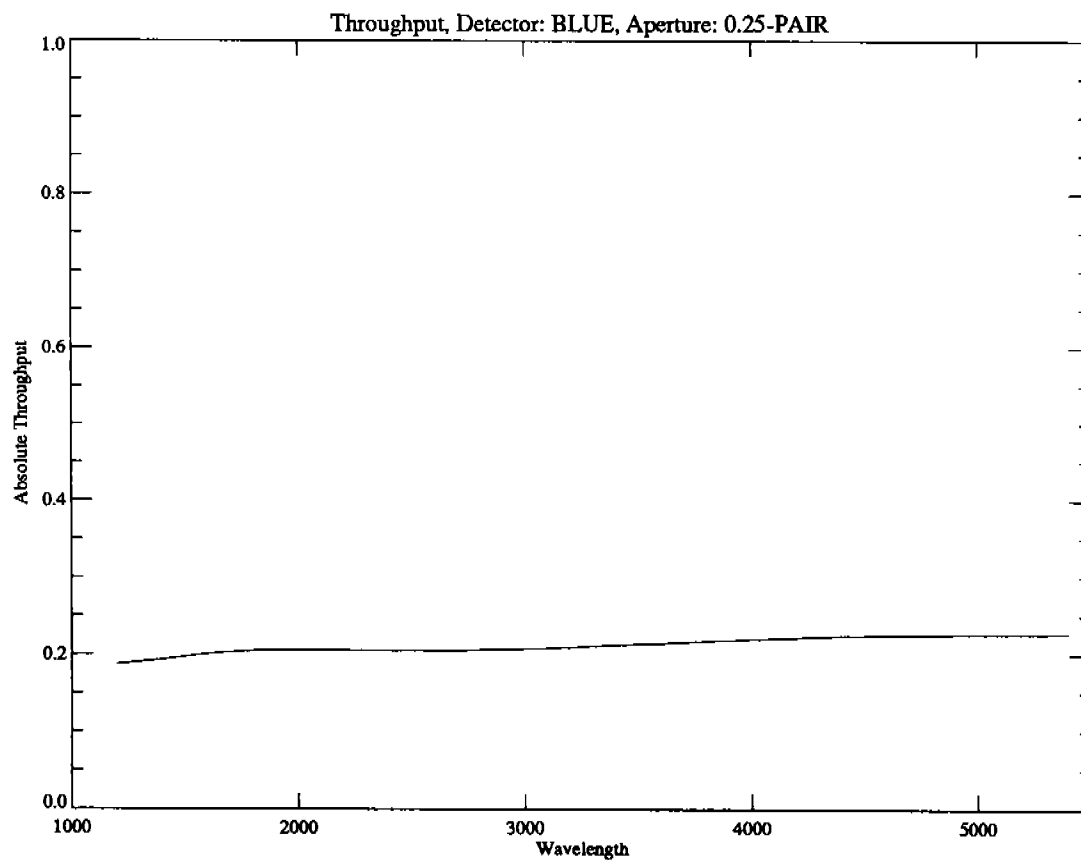
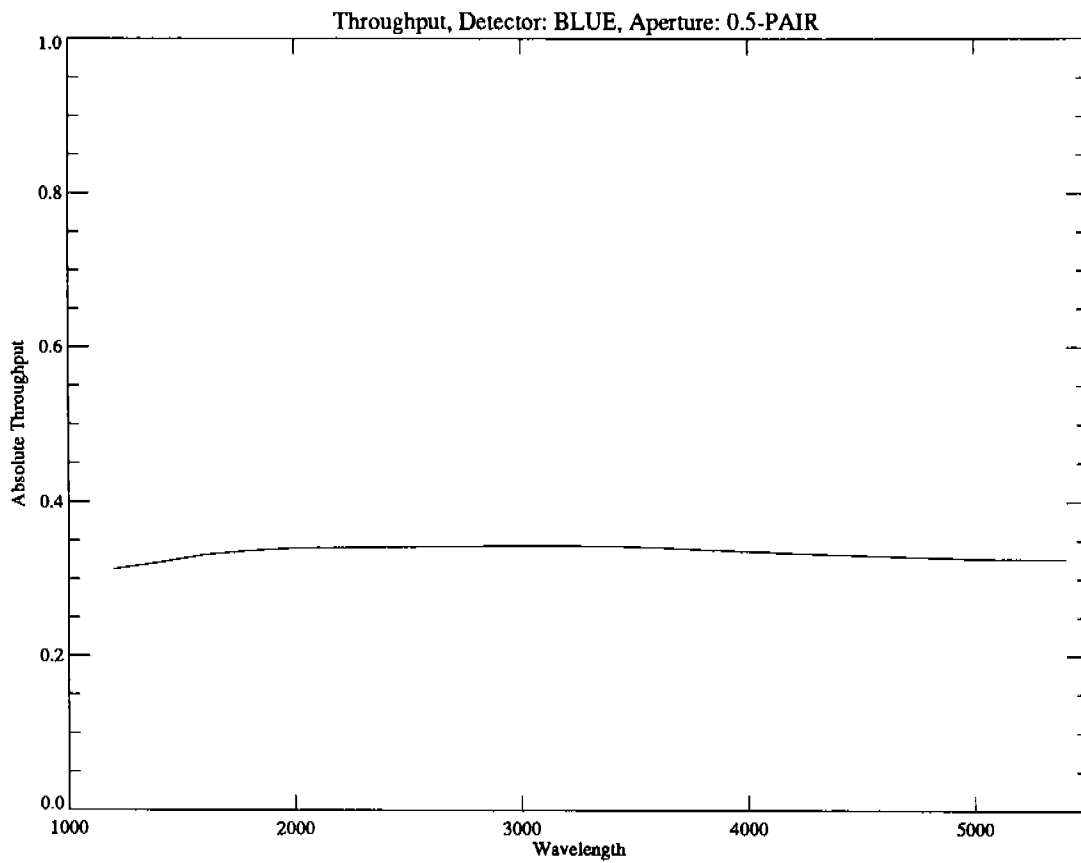


Figure 1 (Continued)

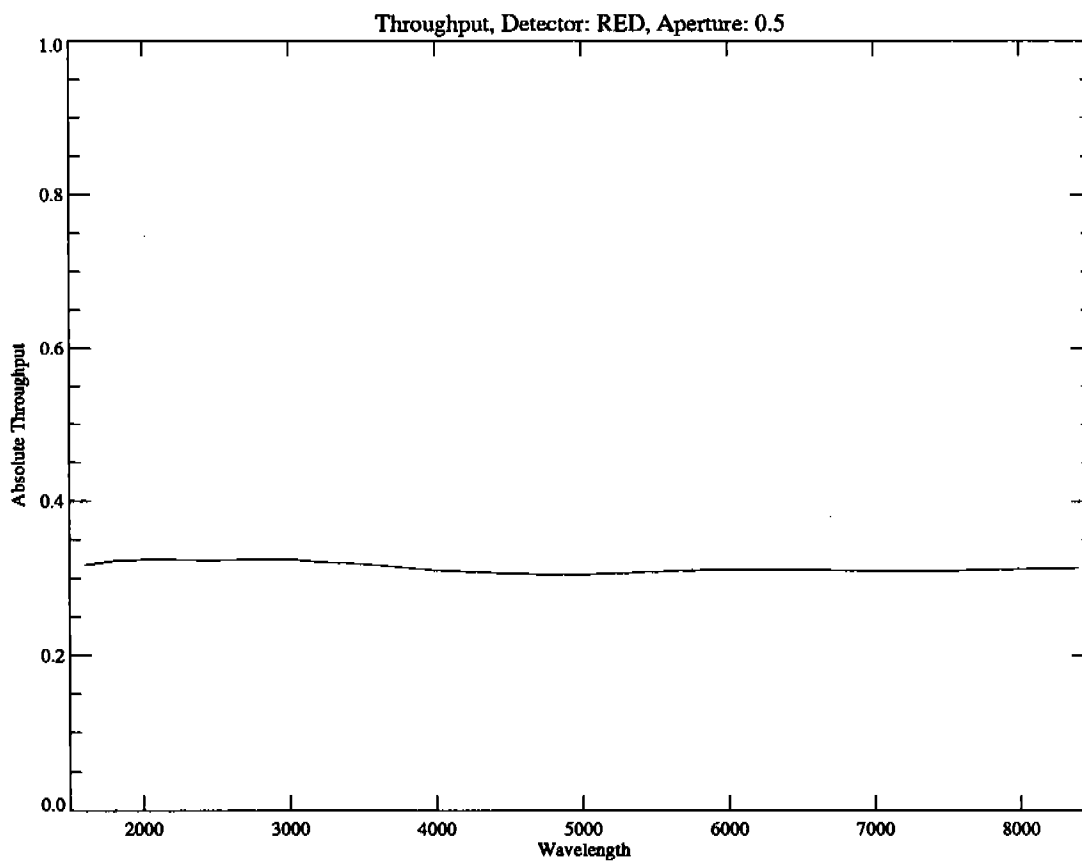
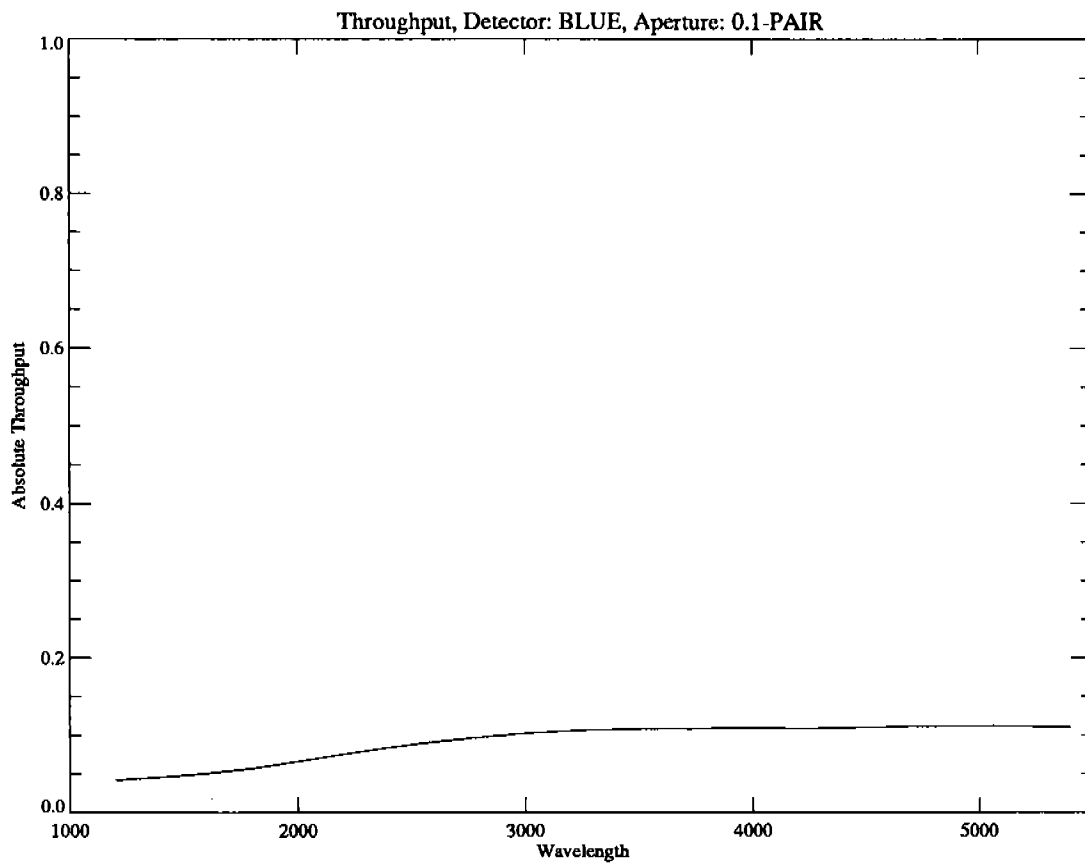


Figure 1 (Continued)

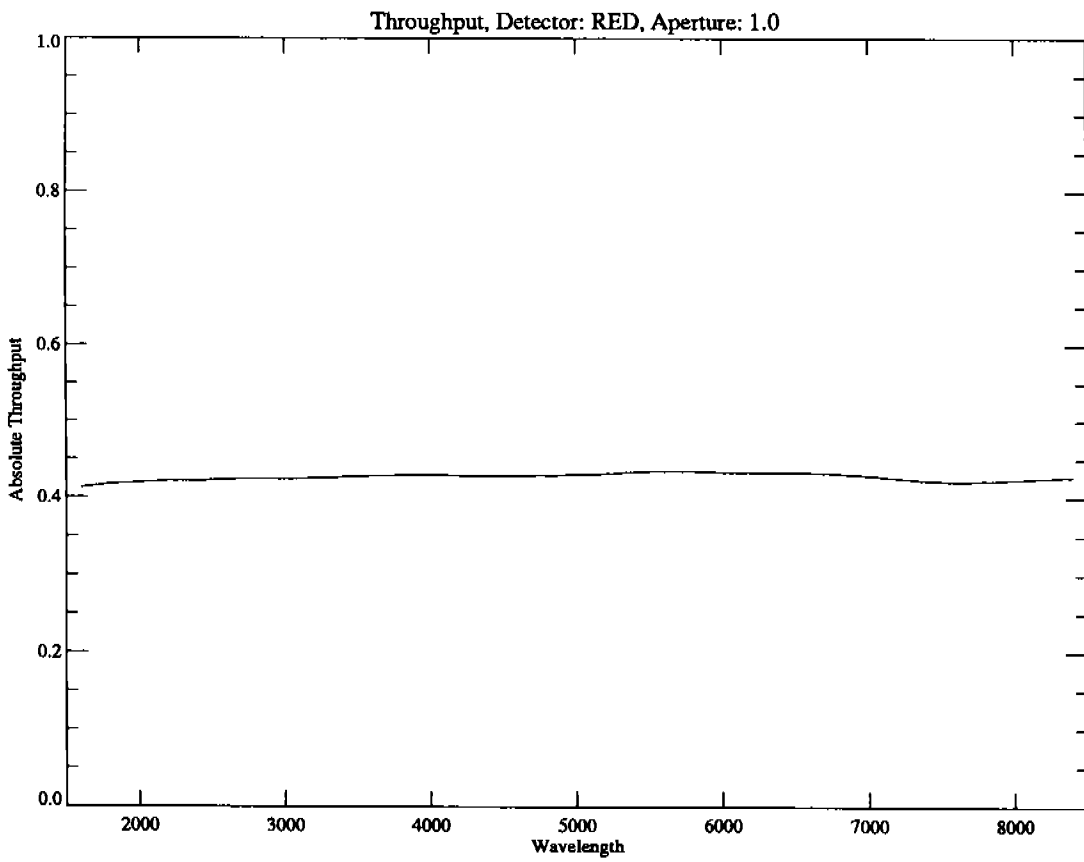
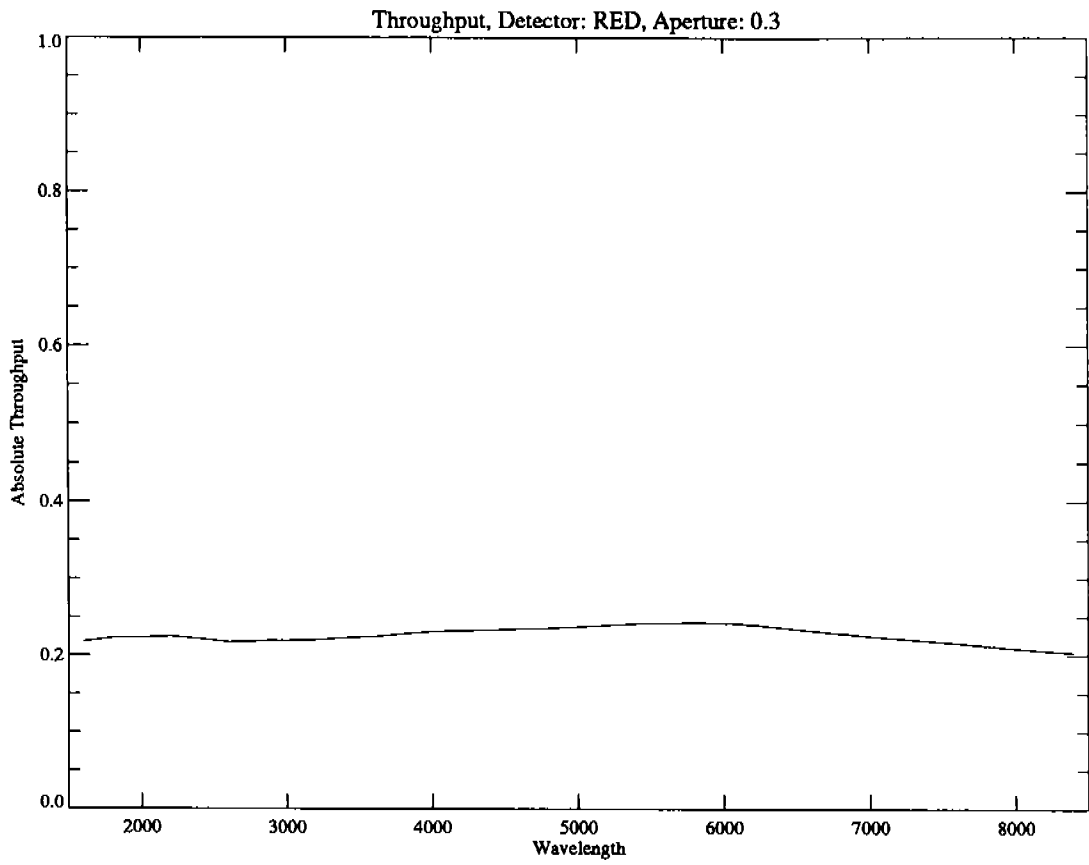


Figure 1 (Continued)

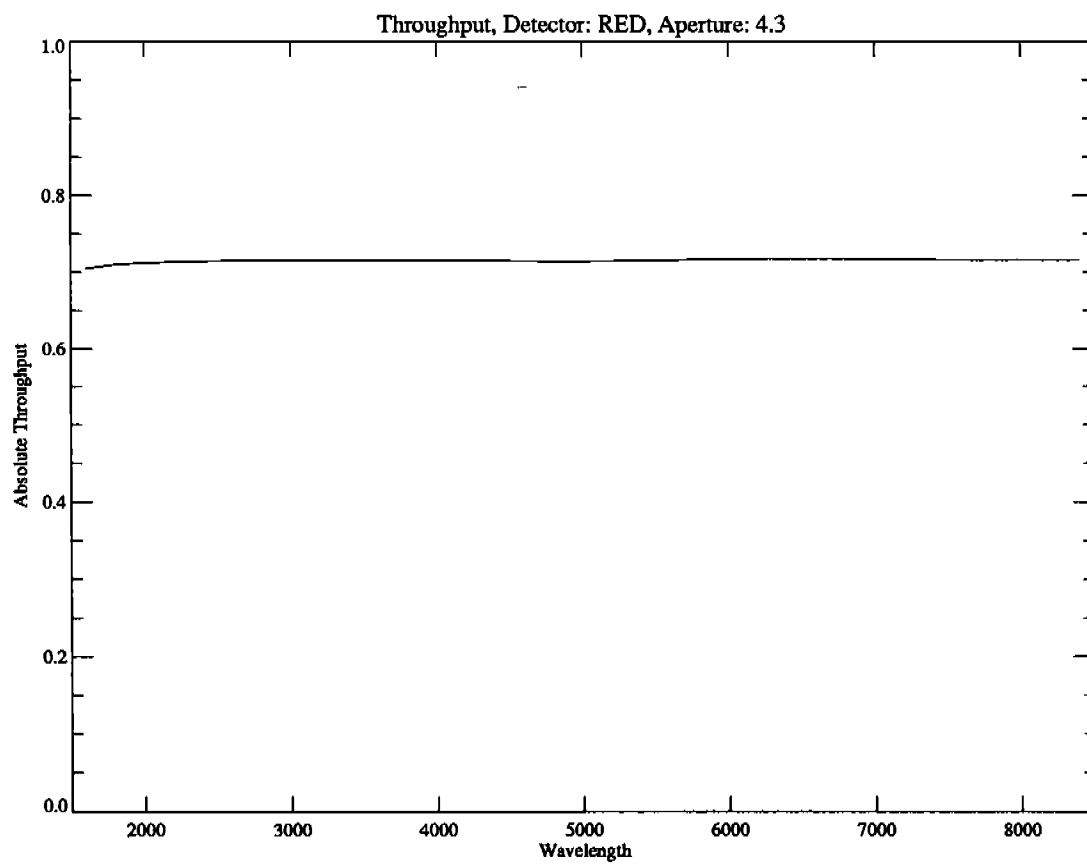
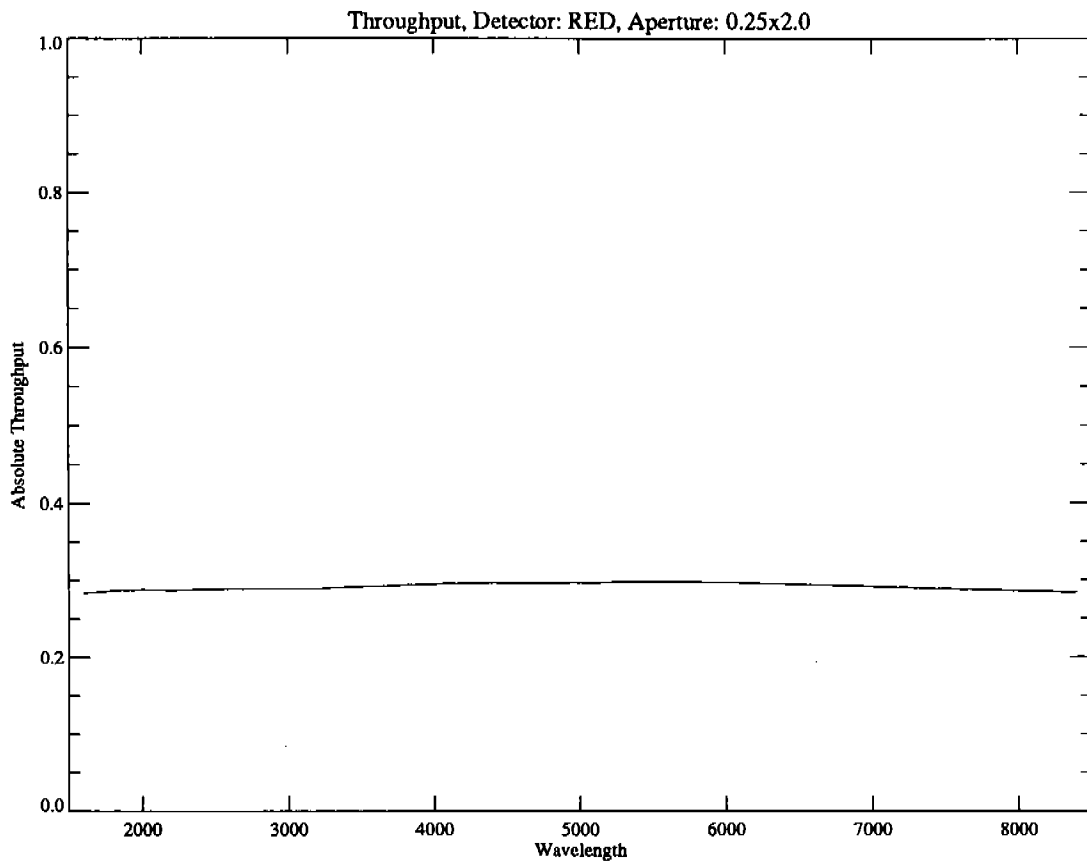


Figure 1 (Continued)

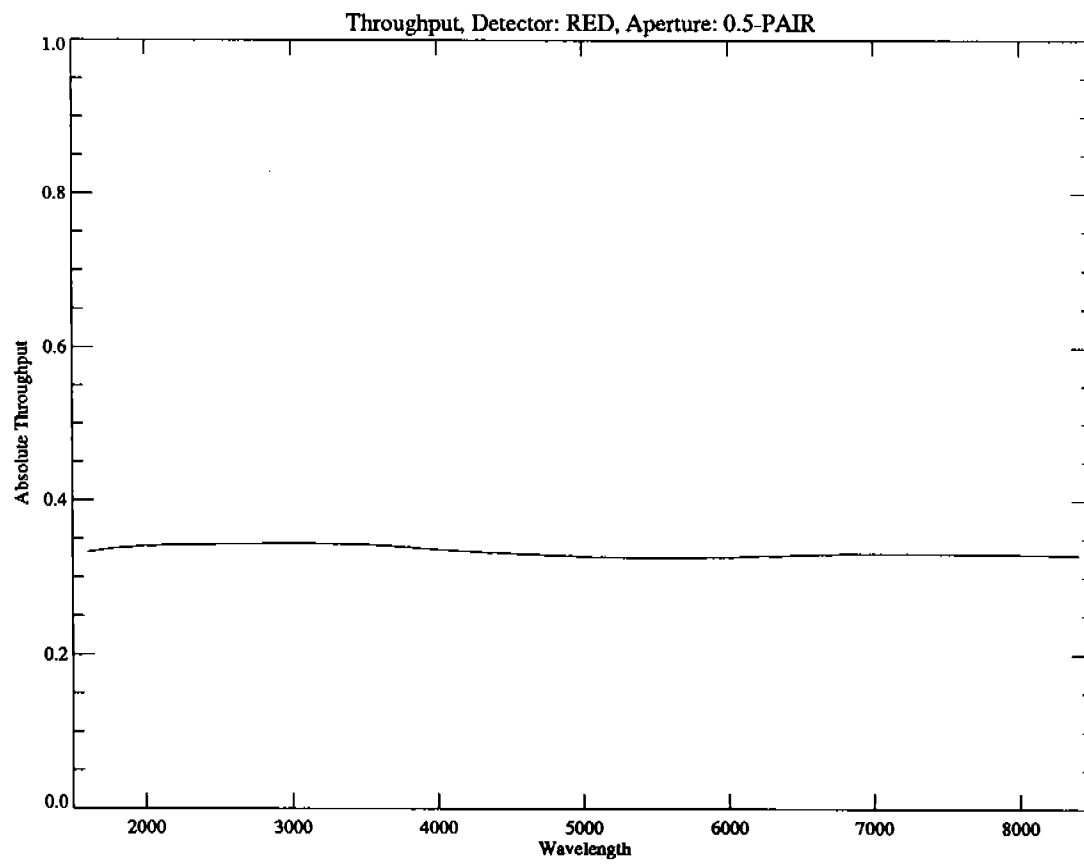
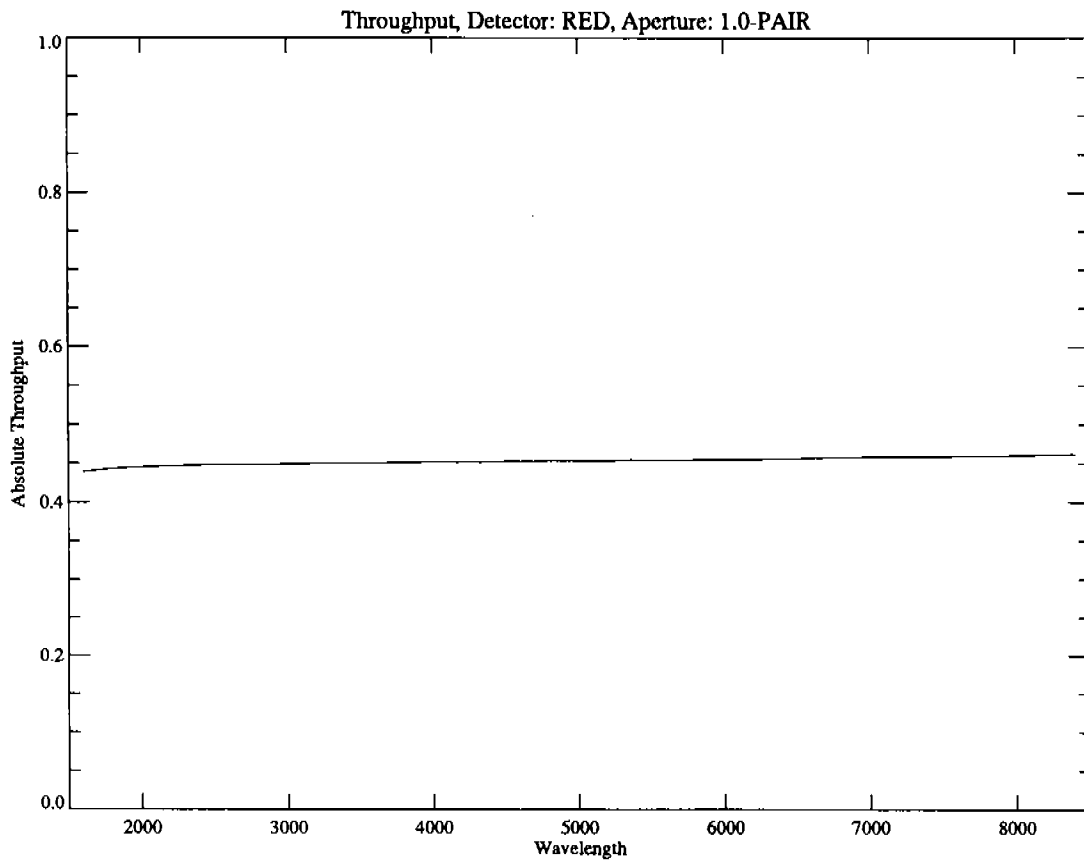


Figure 1 (Continued)

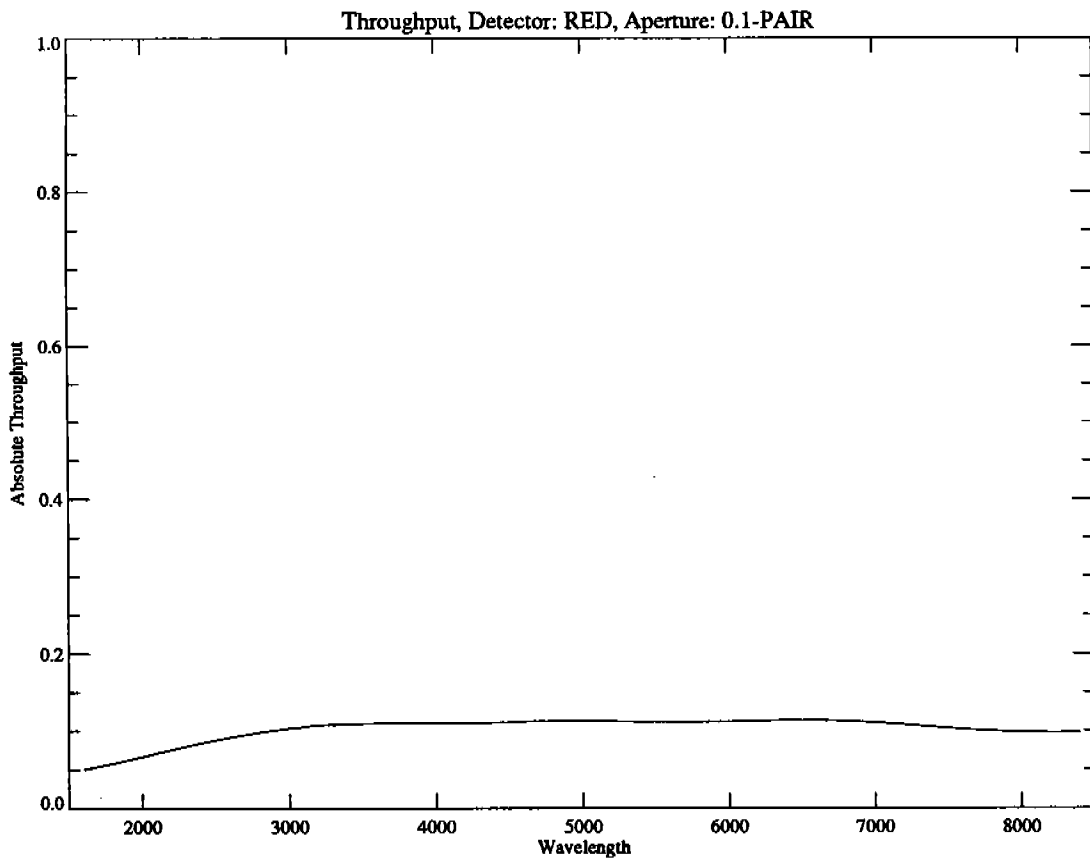
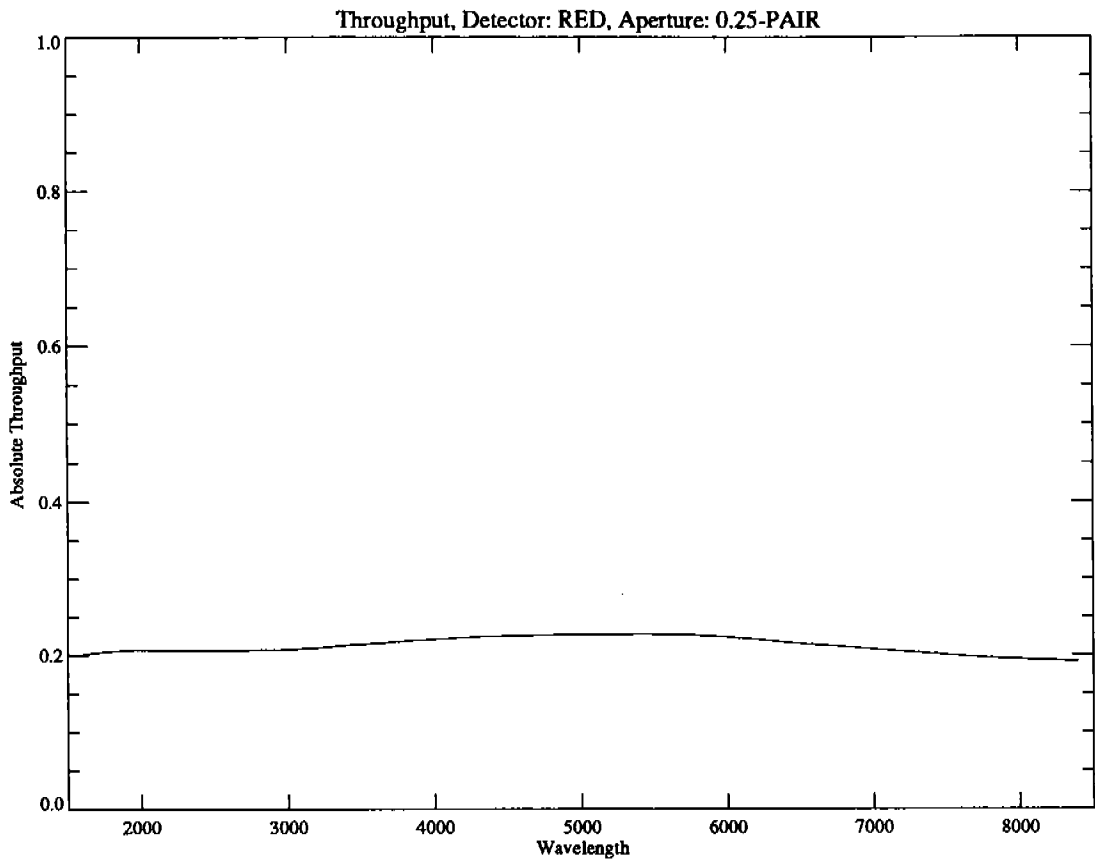


Figure 1 (Continued)

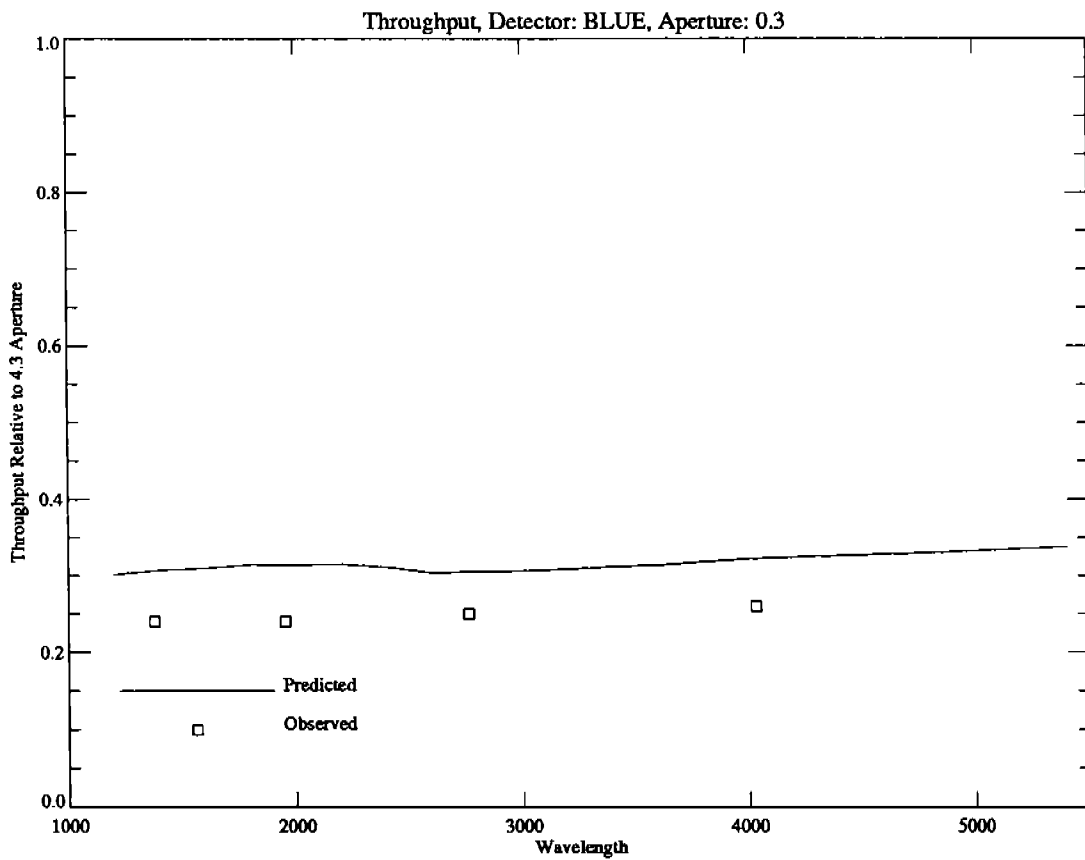
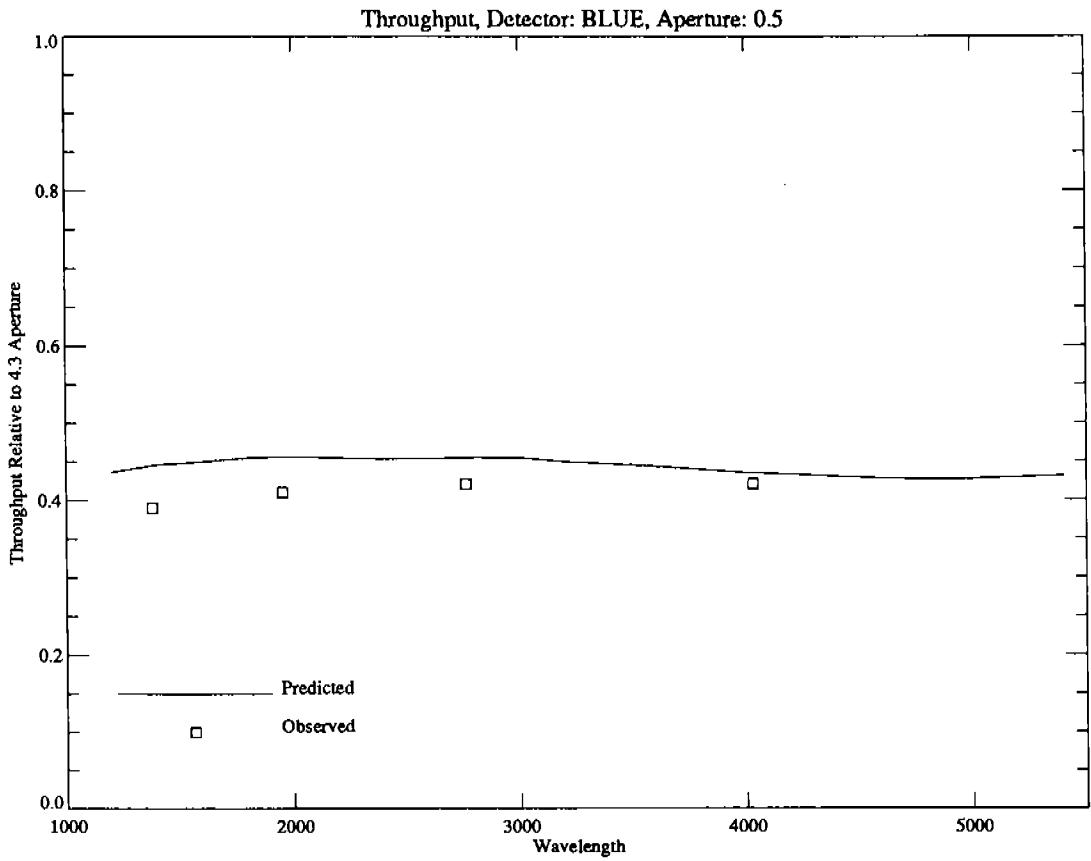


Figure 2

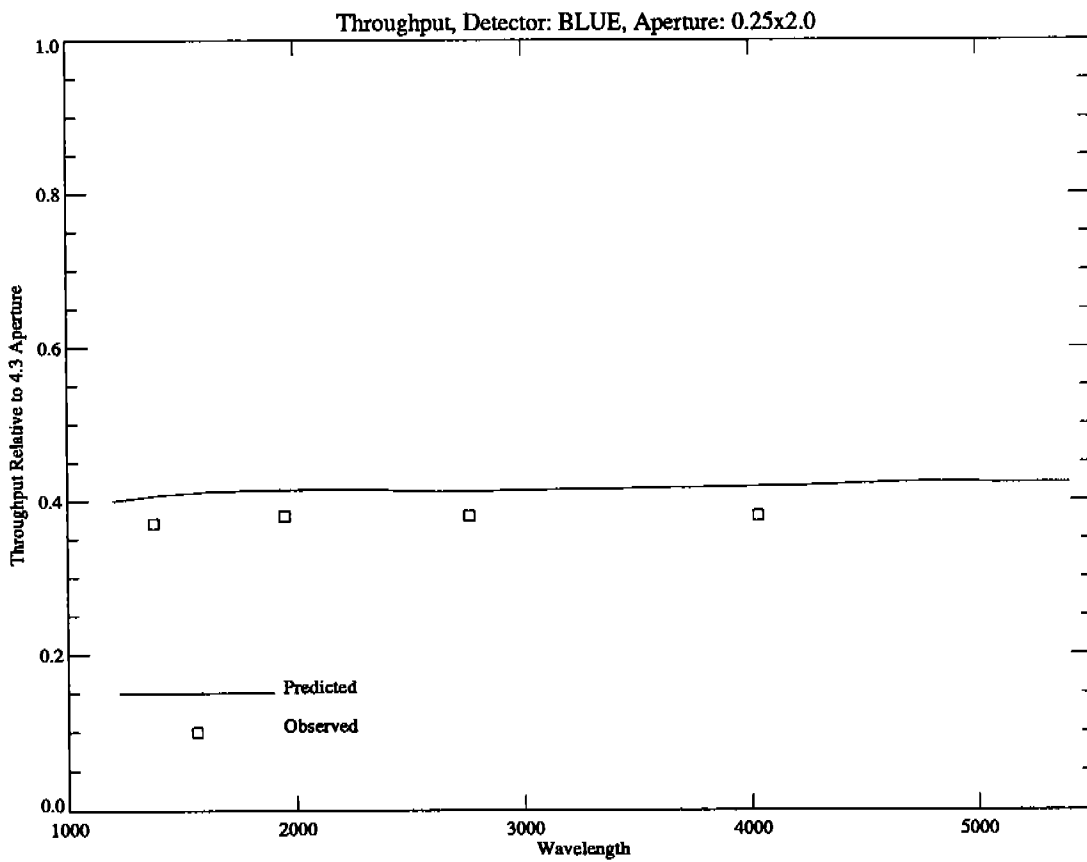
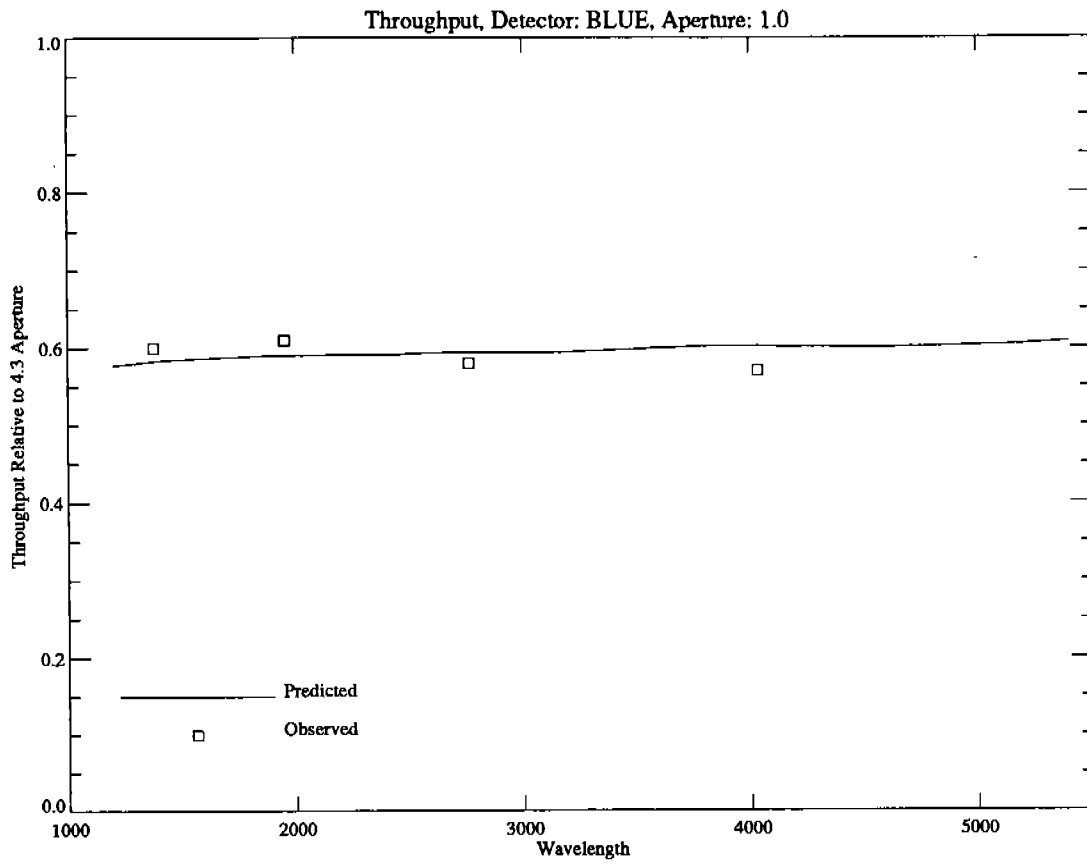


Figure 2 (Continued)

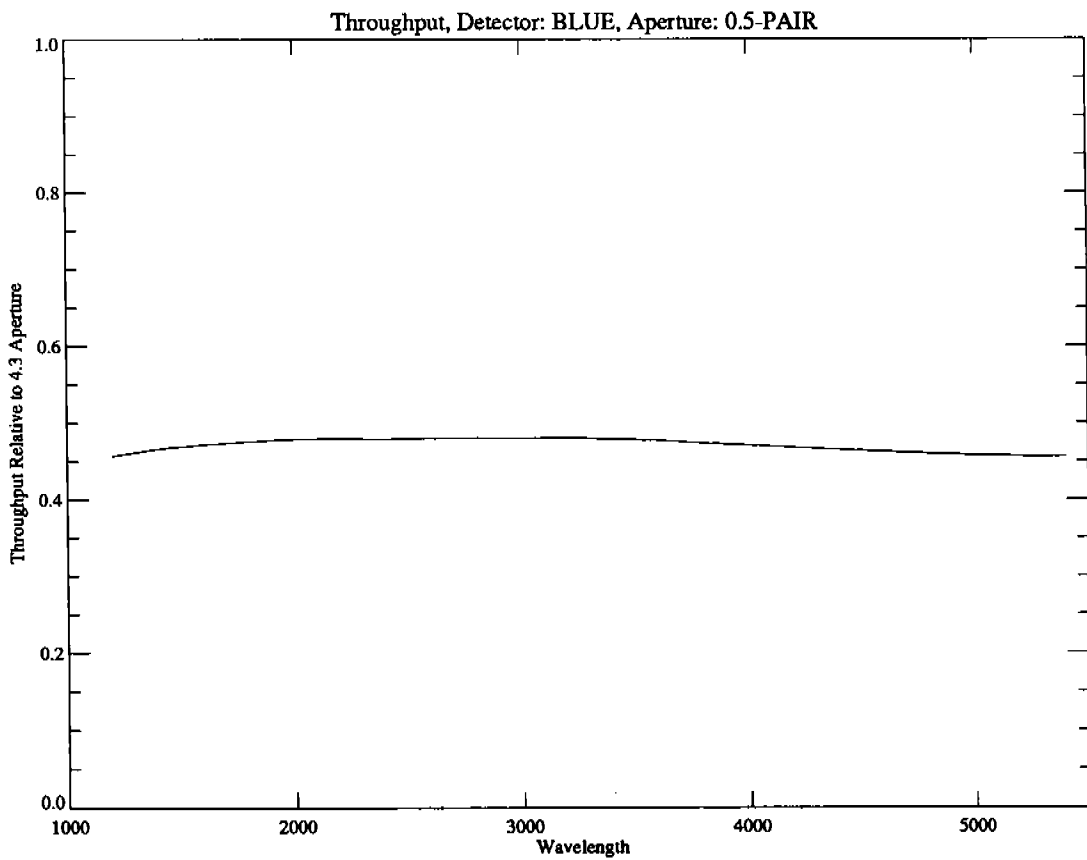
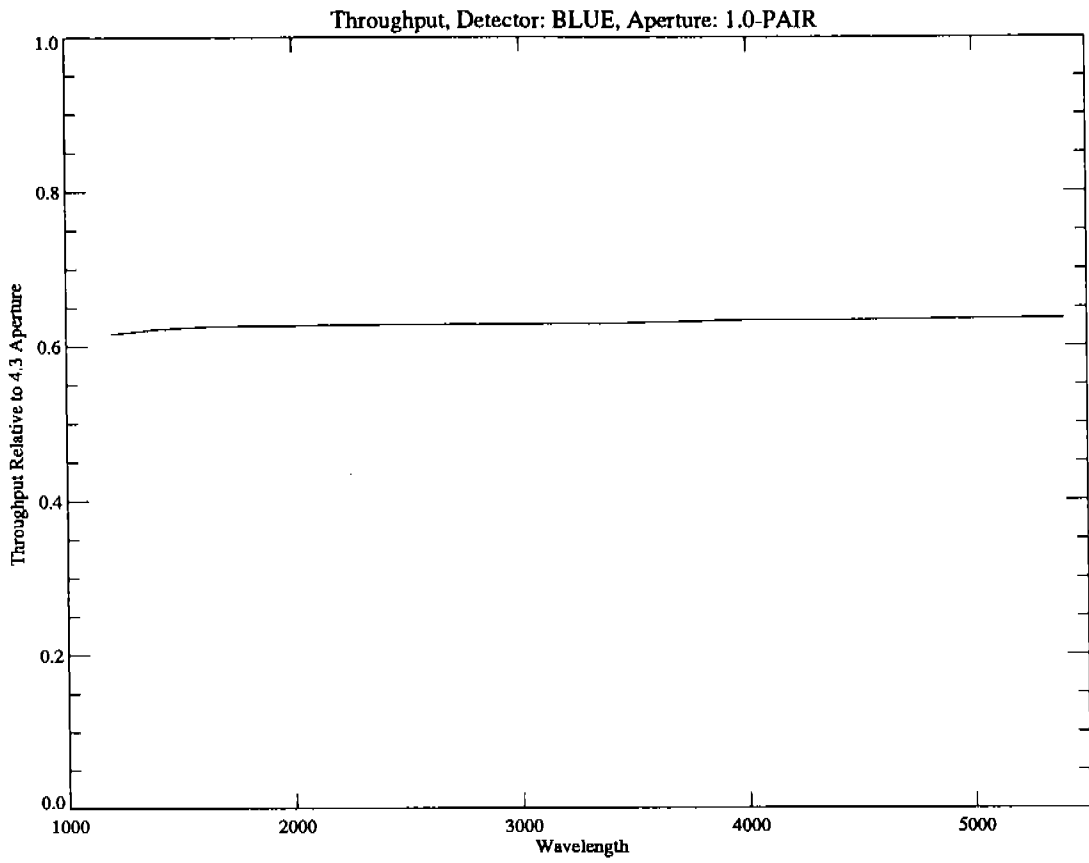


Figure 2 (Continued)

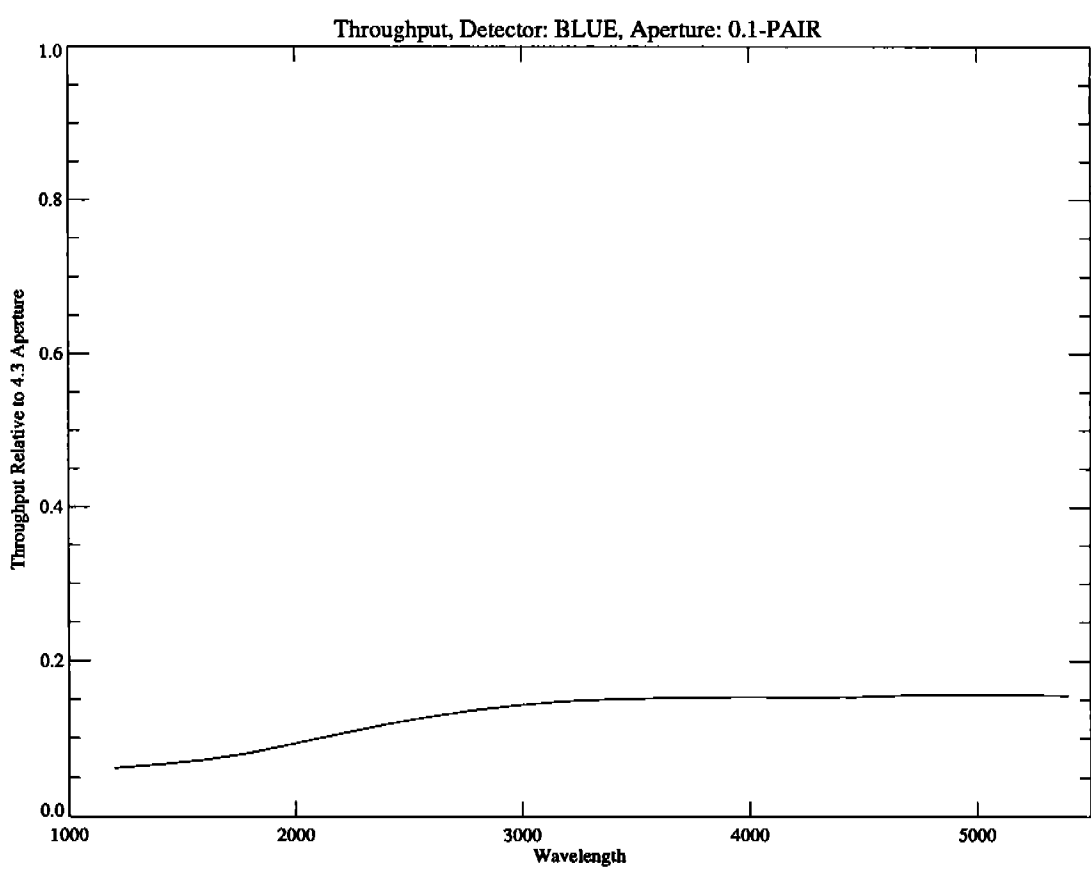
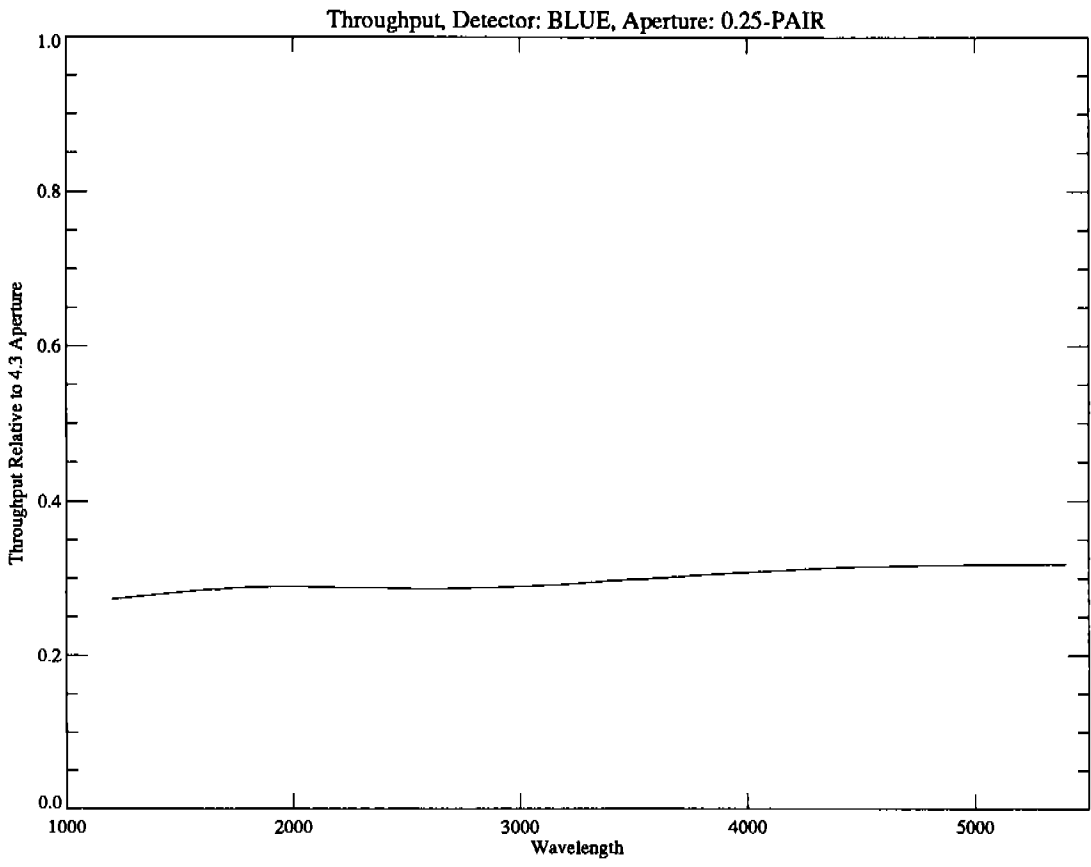


Figure 2 (Continued)

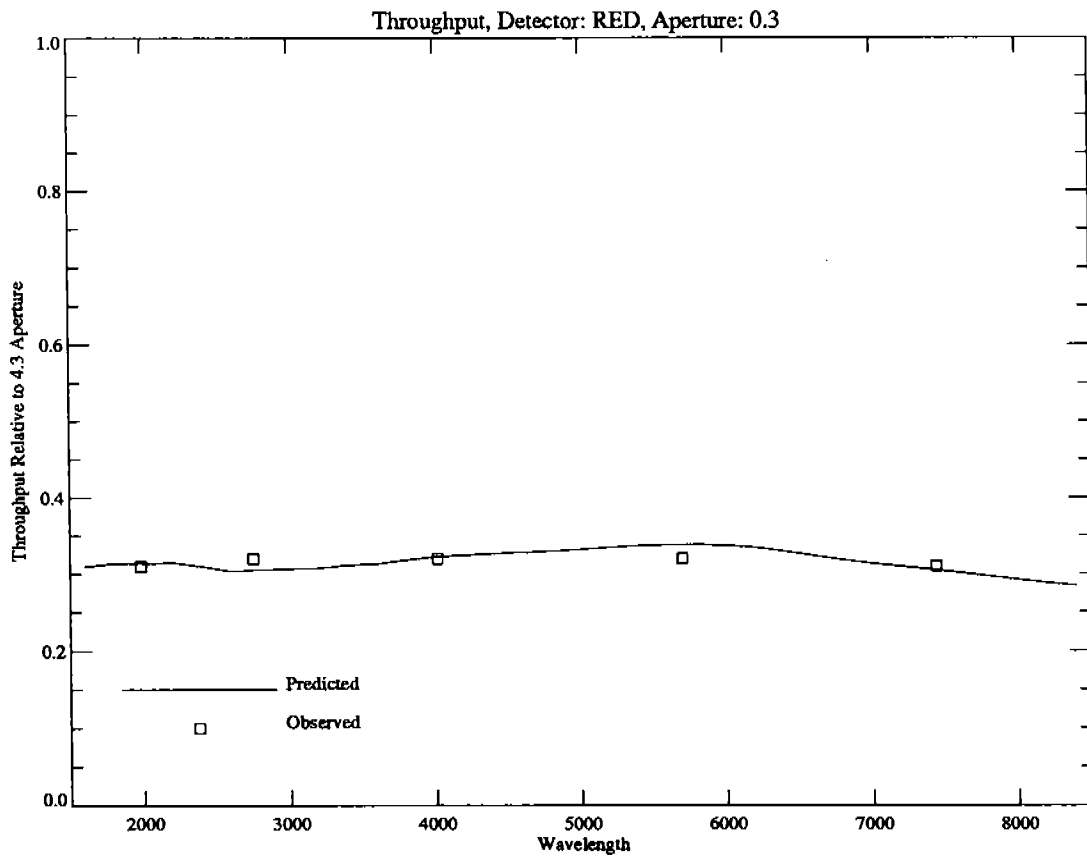
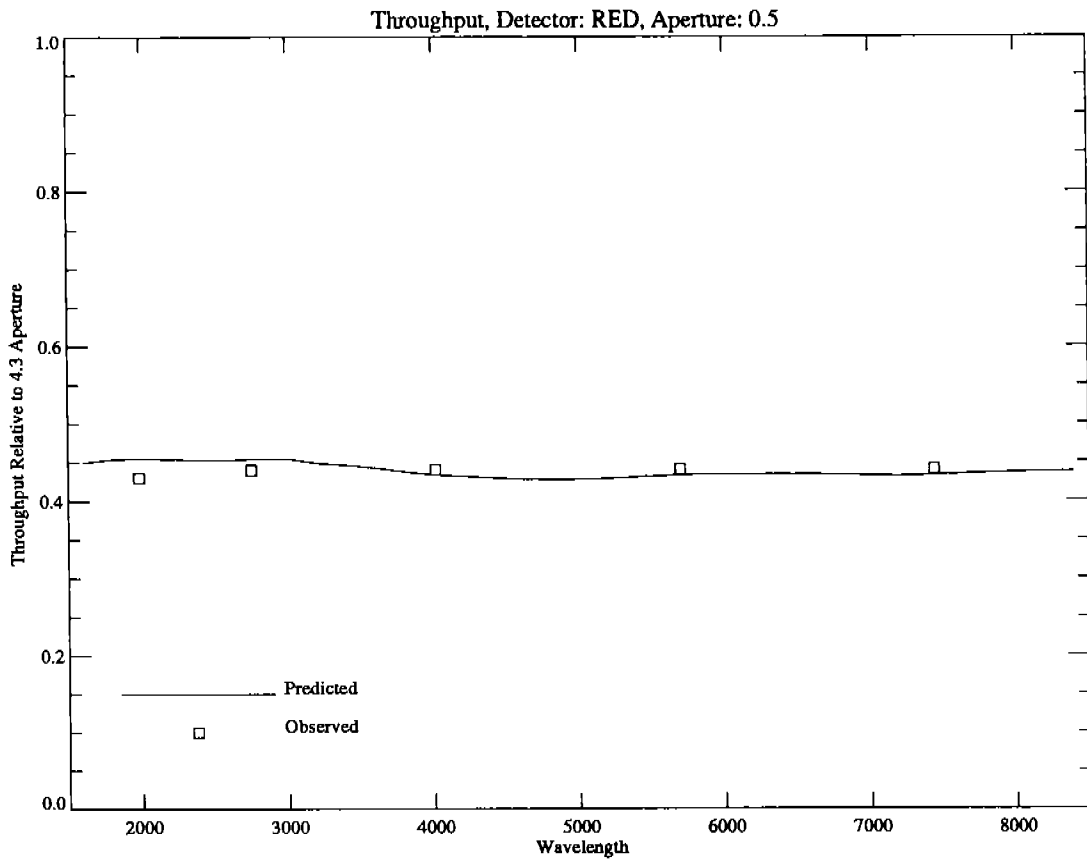


Figure 2 (Continued)

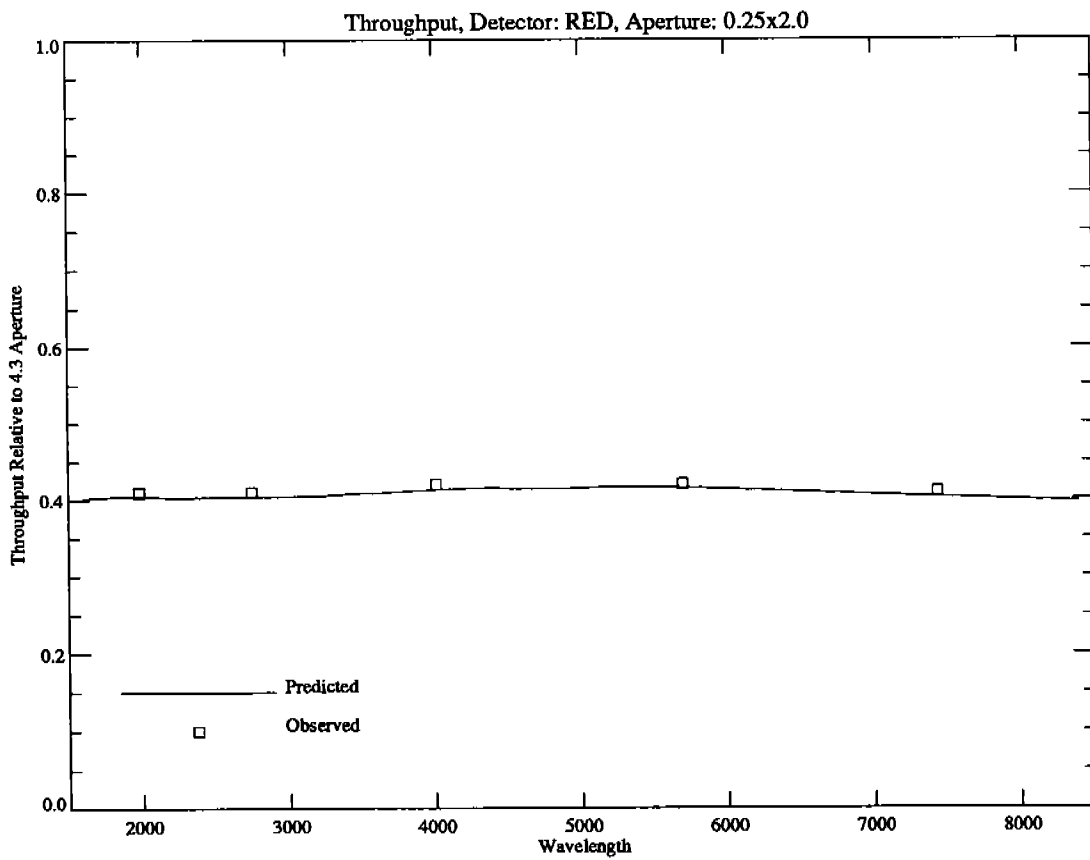
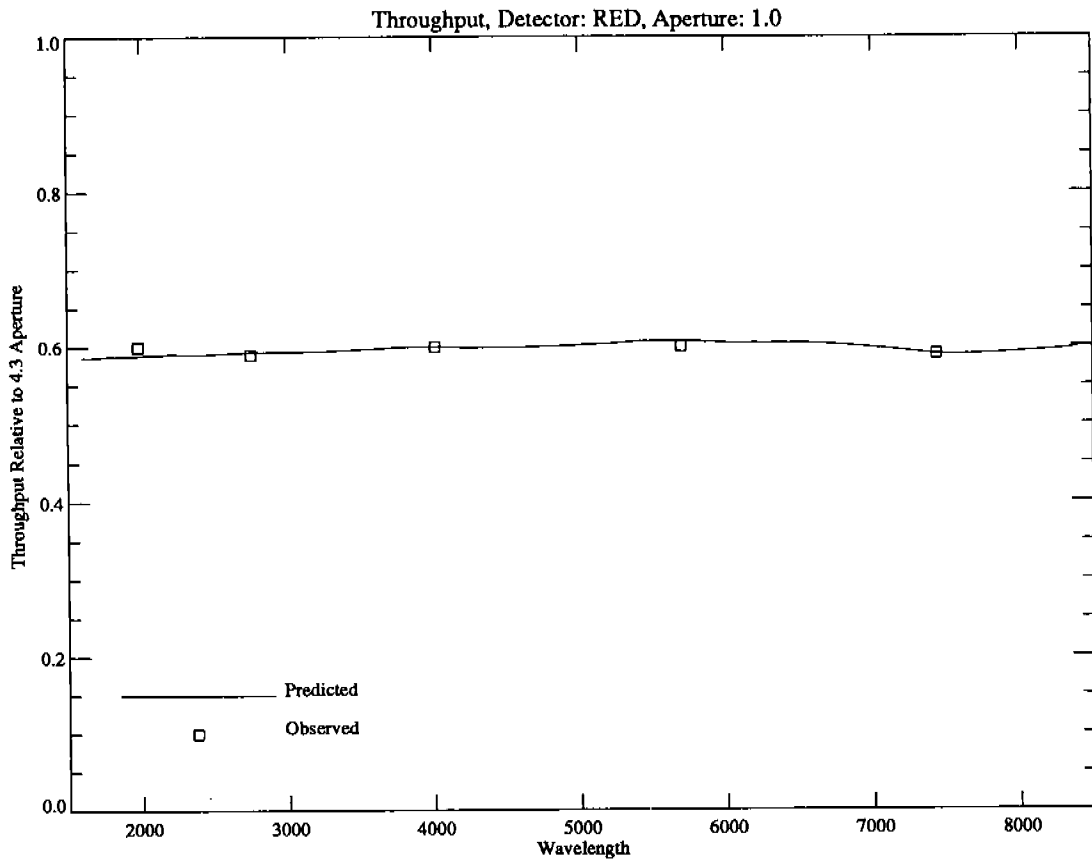


Figure 2 (Continued)

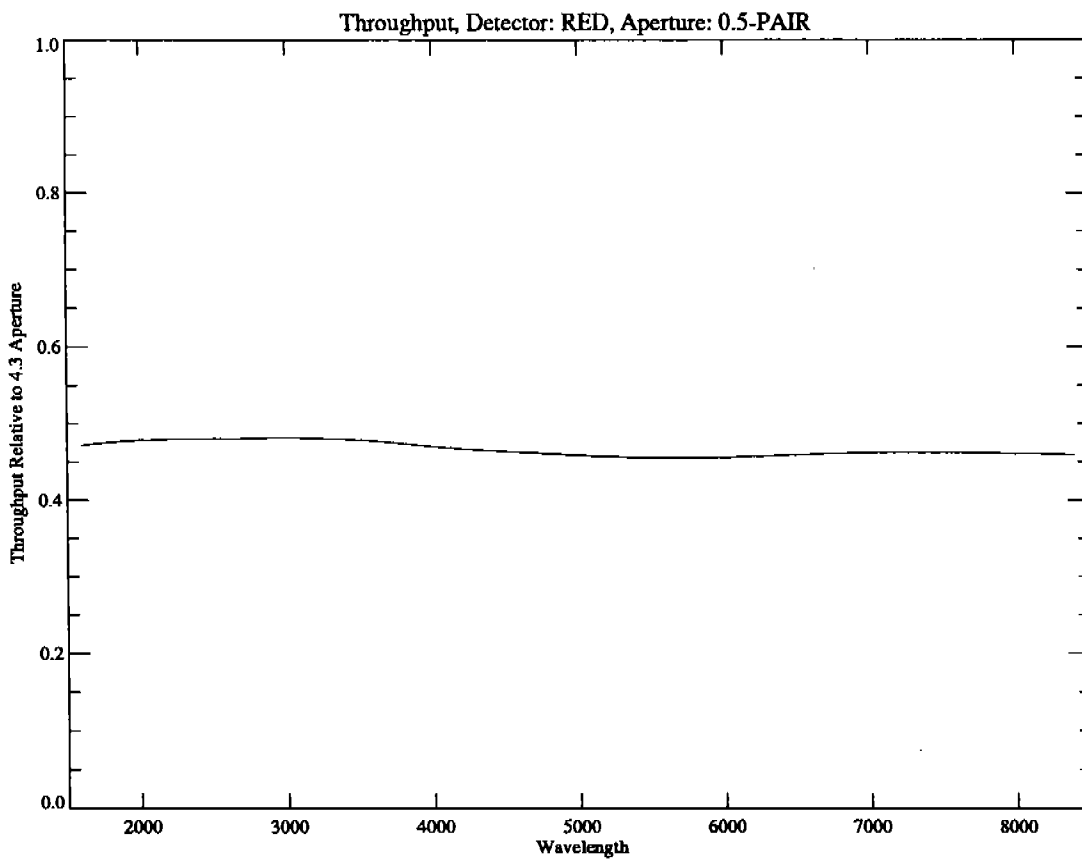
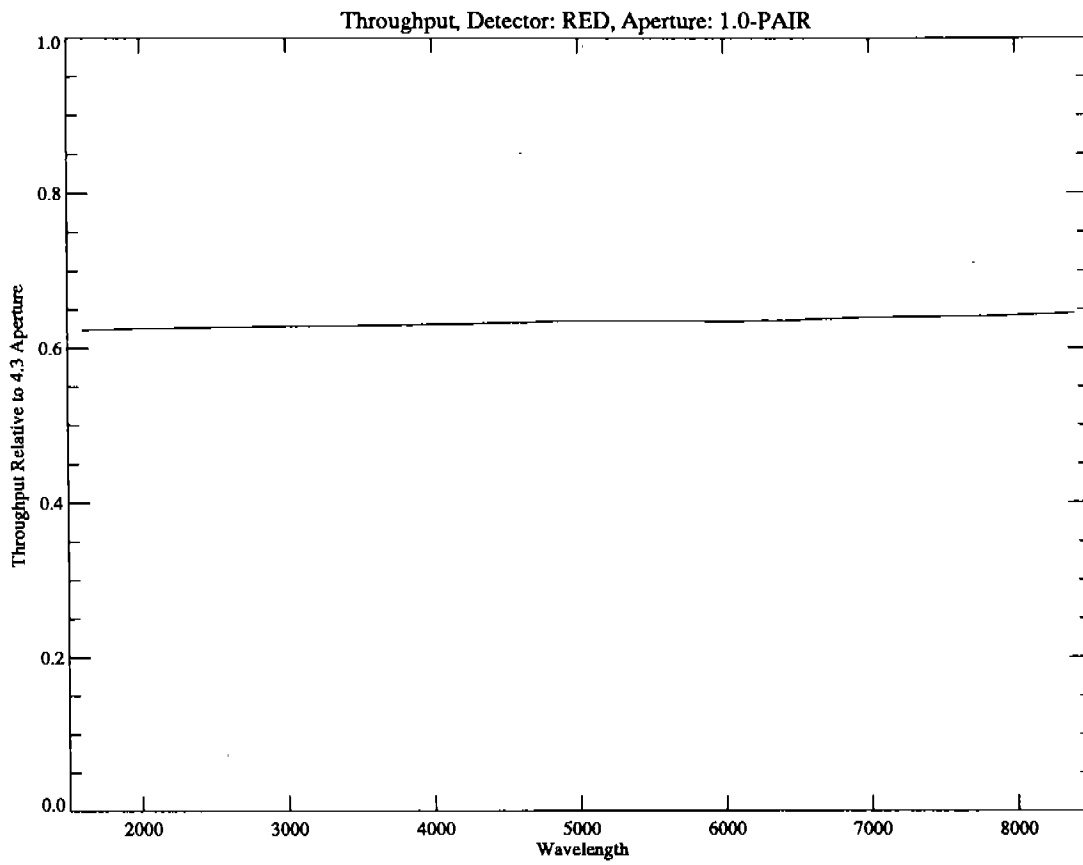


Figure 2 (Continued)

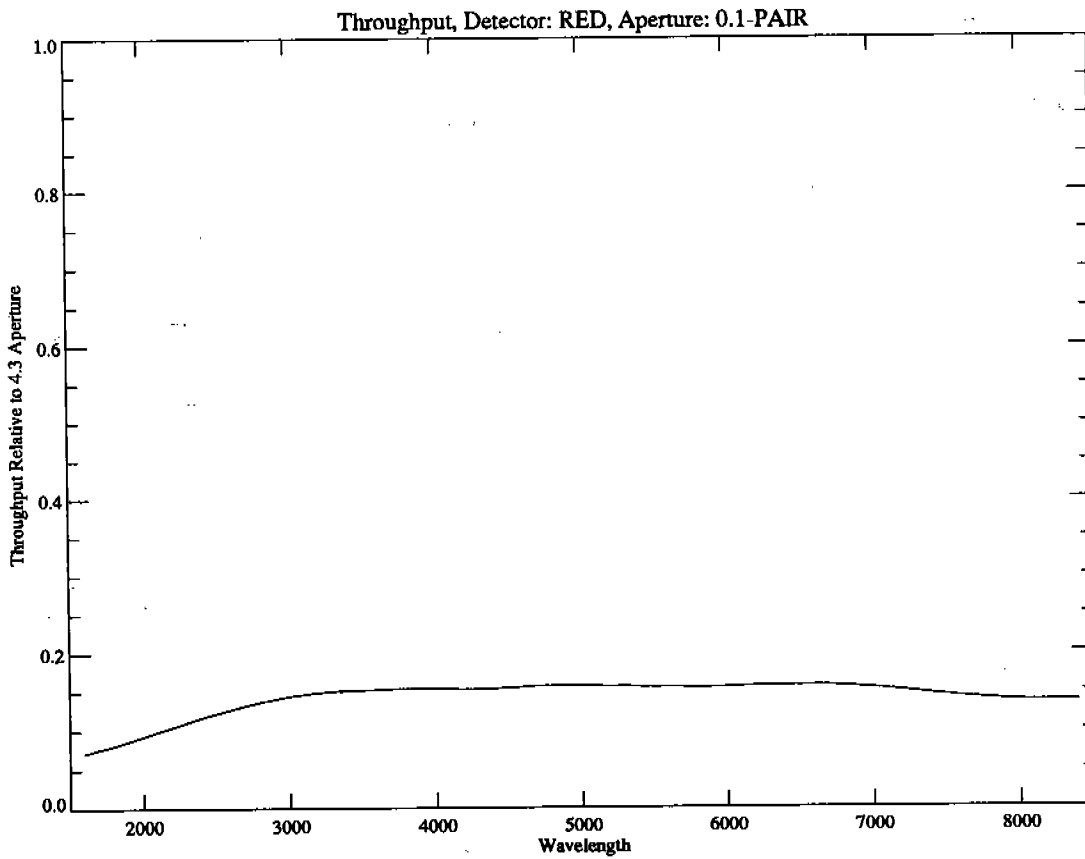
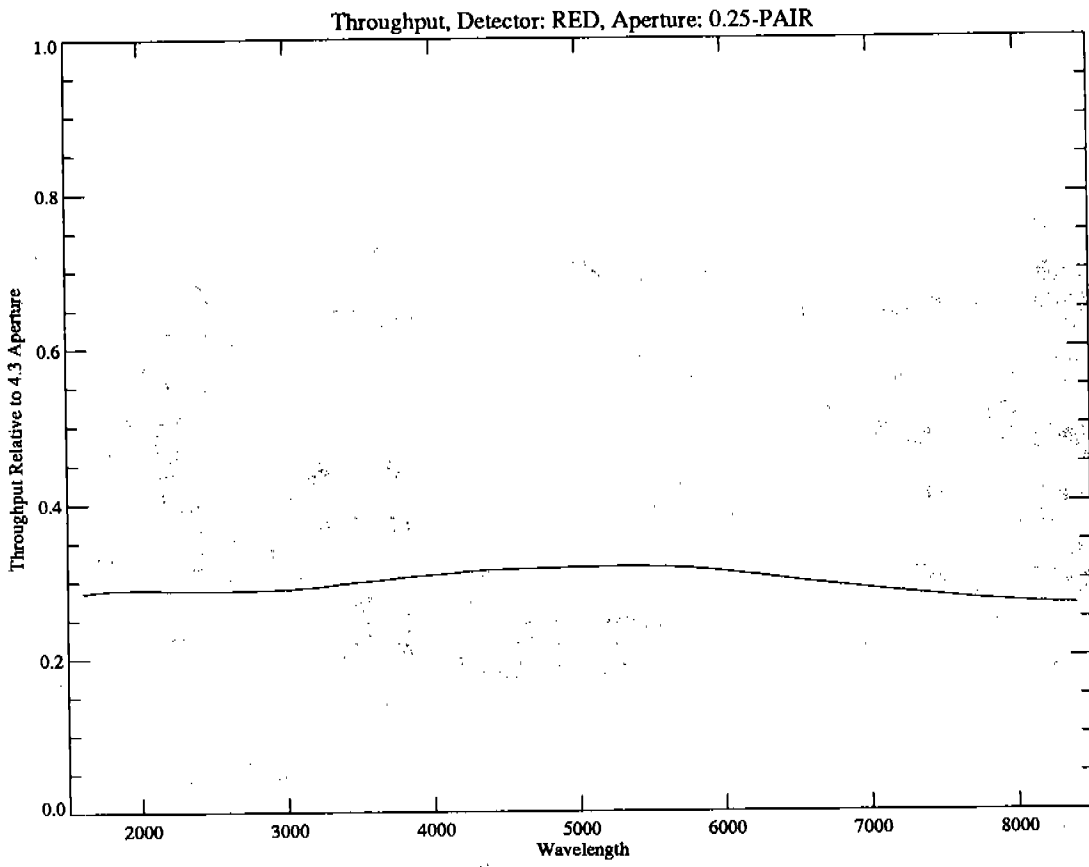


Figure 2 (Continued)